ANSPOLY Journal of Advanced Research in Science &Technology
Volume 1; Issue 1; March 2024

CONTROL AND STABILITY OF A 3 DOF RRR ROBOT ARM

Okonkwo, Ifeanyichukwu Kenneth Jr.
Department of Electrical and Electronics Engineering Technology,
Anambra State Polytechnic, Mgbakwu
Author's E-mail: 27eleven1@gmail.com Tel: 08033534131

Abstract
The mechanical design of the robot arm was illustrated with a CAD drawing and the control goal was stated. A feedback control system for the arm configuration is presented and specifications were given for the design with the servo parameters. Next, the transfer functions of the feedback systems, the process and the controller were modelled. The closed-loop system was a fourth-order system and not a second-order system. So, the controller parameters (a,b, c and K_D) were selected such that two poles are dominant and located appropriately to meet the design specifications/second-order results. The remaining poles of our fourth-order system were located such that their contribution to the overall response was negligible. The appropriate locations for the dominant poles of the closed loop system were determined using second-order system approximation formulae. The step response was plotted and the system was tested using the Nyquist criterion. The results showed that the system was stable and within the specifications.

Keywords: Link, Revolute Joint, End-Effecter, Servo, Degree Of Freedom, Model, Feedback, Loop, Controller, Gain.

1. Introduction
To understand and control complex systems, one must obtain quantitative mathematical models of these systems. It is necessary therefore to analyze the relationships between the system variables and to obtain a mathematical model.

The performance of a feedback system can be described in terms of the location of the roots of the characteristic equation in the s-plane. A graph showing how the roots of the characteristic equation move around the s-plane as a single parameter varies is known as

a root locus plot. The root locus is a powerful tool for designing and analyzing feedback control systems. This is important because we know that the response of a closed-loop feedback system can be adjusted to achieve the desired performance by judicious selection of one or more controller parameters. The PID controller is a popular controller structure widely used in industrial process.

The stability of a feedback system is directly related to the location of the roots of the characteristic equation of the system transfer function. The relative stability and the transient performance of a closed-loop control system are directly related to the location of the closed-loop roots of the characteristic equation in the s-plane. It is frequently necessary to adjust one or more system parameters in order to obtain suitable root locations. Frequency response methods such as the Nyquist stability criterion can be used to investigate stability.

Robot arm modelling and control have received much attention from researchers in the past decades and in recent times. Hossein and Hassan (2014) modeled, simulated and controlled a 3-DOF (deg articulated robot. The model is linearized with feedback and a PID controller is implemented to track a reference trajectory. Farhan (2014) presented a robot arm model based on Simulink. Mathematical, Simulink models and MATLAB program were developed to return maximum numerical visual and graphical data to select, design, control and analyze arm system. In (Okubanjo et al, 2017), the control algorithm is expanded on the derived mathematical equations to control the robot arm in joint angle position. In another paper, “Modeling of 2-DOF Robot Arm and Control”, the control algorithm is expanded on the derived mathematical equations to control the robot arm in joint angle position. The Proportional Integral Derivative (PID) controllers were implemented in the model and the simulation model was developed with the aid of MATLAB and Simulink simulation tool to investigate the system performance in joint space. According to the results analysis, the robot arm was satisfactorily controlled to reach and stay within a desired joint angle position (Okubanjo et al, 2017).In another thesis, “Theory of Robotic Arm Control with PLC” the control system consists of the programmable logic controller (PLC), a motor controller, a voltage regulator, a control pendent and a bride board circuit. The arm works both manually and automatically using

potentiometers and PLC respectively. The complex programming is possible in the PLC for the automatic mode of operation. It is found that a robotic arm with a simple mechanism can be manipulated in a complex way by using a PLC. (Safdar, 2015).

This paper is presented for educational purpose to help beginners glean a wide background of robot arm control.

2.0 Material and Methods

2.1 Design Presentation of the Robot Arm

The robot armis athree revolute joint (RRR) planar armconfiguration which allowsthree independent movements (3 dof). The links are actuated by field-controlled DC servos.

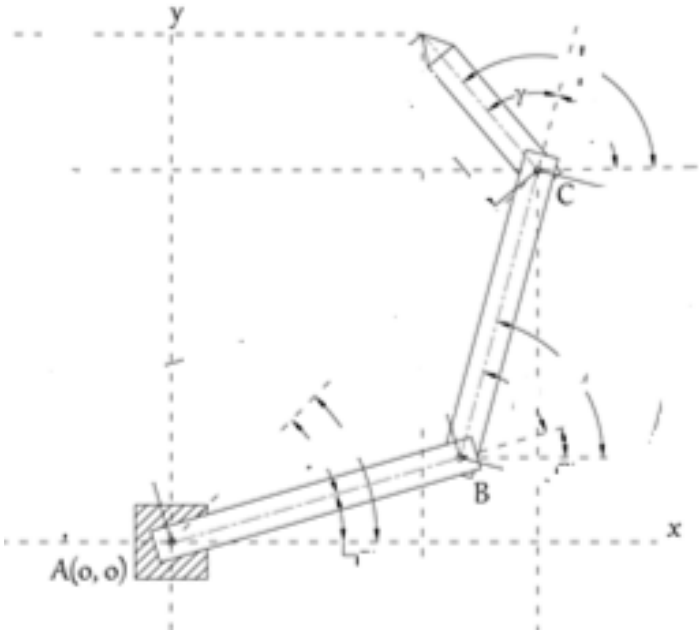

Fig 1: The 3 DOF RRR Planar Robot Arm

2.2 Control Goal

The end-effecter's final position depends on the synchronous movements of all the joints of the arm. The aim is to place the tip of the tip of the end-effecter at the commanded position with minimal overshoot by controlling the rotation of each joint through required path lengths till its corresponding link is properly configuredis properly configured in the presence of disturbances.

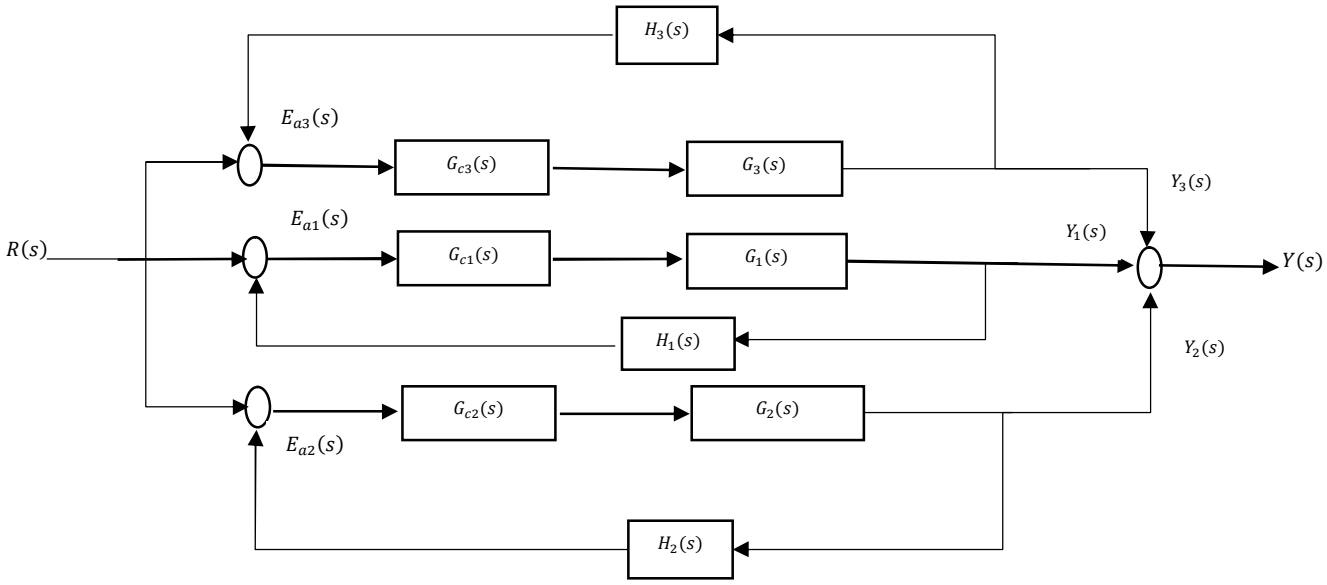

Fig. 2 Control System for the Robot Arm

Each loop represents a joint and the immediate link it carries We shall focus our attention on each loop.

2.3 Design Specifications

Closed-loop bandwidth greater than 1Hz.
A settling time to within 2% of the final value of less than 2 seconds.
Percent overshoot less than 15 percent to a step input.
Input voltage,$R(s) = 4.8v$

Angular velocity of the field controlled DC servo at each jointfor $4.8v$supply,$\varpi(s) = {d\theta}/{dt} = 63.65°/s$

Field time constant $\tau_f = 0.02$sec
Mechanical time constant $\tau_L = 2$sec

For feedback, a potentiometer is used as the position sensor with ±2.4v between two end terminals and measure the voltage of the brush relative to the ground. Since one revolution gives a voltage change of 4.8v, the sensor gain is 4.8v per revolution.

2.4 Modelling

2.4.1 System Transfer Functions, $\boldsymbol{T(s)}$

The system output is

$$Y(s) = \frac{G_{c1}(s)G_1(s)}{1 + L_1(s)}R(s) + \frac{G_{c2}(s)G_2(s)}{1 + L_2(s)}R(s) + \frac{G_{c3}(s)G_3(s)}{1 + L_3(s)}R(s) \tag{1}$$

The transfer function of the three-link arm is thus

$$T_3(s) = \frac{G_{c1}(s)G_1(s)}{1 + L_1(s)} + \frac{G_{c2}(s)G_2(s)}{1 + L_2(s)} + \frac{G_{c3}(s)G_3(s)}{1 + L_3(s)} \tag{2}$$

The same controller is used in every loop and the same dynamic process occurs in every loop, so we put

$$\boldsymbol{T_3(s) = 3\frac{G_c(s)G(s)}{1 + L(s)}} \tag{3}$$

and with unitary feedback in all loops, the loop gain for every loop is thus

$$\boldsymbol{L(s) = G_c(s)G(s)H(s) = G_c(s)G(s)} \tag{4}$$

Thus

$$\boldsymbol{T_3(s) = 3\frac{L(s)}{1 + L(s)}} \tag{5}$$

and the closed loop transfer function of every loop (each joint/link of the robot arm) is

$$\boldsymbol{T_1(s) = \frac{L(s)}{1 + L(s)}} \tag{6}$$

2.4.2 Process Transfer Function of the Actuator/Link (Field Controlled DC Servo), $\boldsymbol{G(s)}$

The transfer function of a D.C. Servomotor is given as

$$G_\theta(s) = \frac{K_m/bR_f}{s(\tau_f s + 1)(\tau_L s + 1)} = \frac{K}{s(\tau_f s + 1)(\tau_L s + 1)} \tag{7}$$

We need to determine the gain K but K_m, b and R_f are not included in the motor specifications but we have that $\varpi(s) = 63.65^o/s$ and $R(s) = 4.8v$. Thus, we can use the transfer function, $G(s)$ from the field voltage V_f to the shaft angular velocity ϖ and compare with $G_\theta(s)$ in eq.(7)to deduce K.

$$G(s) = \frac{\varpi(s)}{V_f(s)} \tag{8}$$

To convert $G_\theta(s)$ to $G(s)$ the Laplace integral operator $1/s$ in $G_\theta(s)$ is differentiated out.

Now comparing,

$$G(s) = \frac{\varpi(s)}{V_f(s)} = \frac{K}{(\tau_f s + 1)(\tau_L s + 1)} \tag{9}$$

Putting $\varpi = 63.65^o/s \equiv 1.111\ rad/s$ and $V_f = 4.8v$ we have

$$0.23 = \frac{K}{(\tau_f s + 1)(\tau_L s + 1)}$$

Using final value theorem of the Laplace transform,

$$0.23 = \lim_{s \to 0} \frac{K}{(\tau_f s + 1)(\tau_L s + 1)}$$

$$K = 0.23$$

With $K = 0.23$, $\tau_f = 0.02$sec and $\tau_L = 2$sec, $G(s)$ can now be written using eq. (9) as

$$\boldsymbol{G(s) = \frac{0.23}{0.04s^3 + 2.02s^2 + s}} \tag{10}$$

2.4.3 Transfer Function of the Controller, $G_c(s)$

Let the controller be of the form

$$\boldsymbol{G_c(s) = \frac{K_D s^2 + K_P s + K_I}{s + c}} \tag{11}$$

As $c \to 0$, a proportional-integral-derivative (PID) controller is obtained where K_D, $K_P$and K_I are the controller gains.

Putting$K_P = K_D a$and $K_I = K_D b$, $G_c(s)$ can be written in terms of $K_D$as

$$G_c(s) = \frac{K_D(s^2 + as + b)}{\mathrm{s} + \mathrm{c}} \tag{12}$$

This controller introduces a transfer function with two zeros anywhere on the *s*-plane (see the quadratic numerator) and one pole at the origin. The key tuning parameters a,b and $K_D$should satisfy design specifications.

Using this controller, the loop gain is

$$L(s) = G(s)G_c(s) = \frac{0.23(K_D s^2 + K_D as + K_D b)}{0.04s^4 + (2.02 + 0.04c)s^3 + (2.02c + 1)s^2 + cs} \tag{13}$$

and the closed loop transfer function of every loop is

$$T_1(s) = \frac{0.23(K_D s^2 + K_D as + K_D b)}{0.04s^4 + (2.02 + 0.04c)s^3 + (2.02c + 1 + 0.23K_D)s^2 + (c + 0.23K_D a)s + 0.23K_D b} \tag{14}$$

Our closed-loop system is a fourth-order system and not a second-order system. So, a valid design approach would be to select the controller parameters (a,b and K_D) such that two desired dominant poles are located appropriately to meet the design specifications and second-order results. The remaining poles of our fourth-order system are located such that their contribution to the overall response is negligible.

The closed-loop transfer function has the characteristic equation:

$$s^4 + (50.5 + c)s^3 + (50.5c + 25 + 5.75K_D)s^2 + (25c + 5.75K_D a)s + 5.75K_D b = 0 \quad (15)$$

Let the desired characteristic equation, be composed of multiple factors as

$$(s^2 + 2\zeta\omega_n s + {\omega_n}^2)(s^2 + d_1 s + d_0) = 0 \quad (16)$$

such that the roots of $s^2 + 2\zeta\omega_n s + {\omega_n}^2 = 0$are the dominant roots (where ζ and ω_n are selected to meet the design specifications) while the roots of $s^2 + d_1 s + d_0 = 0$are the non-dominant roots.

For $s^2 + 2\zeta\omega_n s + {\omega_n}^2 = 0$,the dominant roots should lie on a vertical line in the complex plane defined by the distance $s = -\zeta\omega_n$ away from the imaginary axis. Considering $s^2 + d_1 s + d_0 = 0$,if we let $d_1 = 2\alpha\zeta\omega_n$, the non-dominant roots when complex, lie on a vertical line in the complex plane defined by $s = -\alpha\zeta\omega_n$. If α>1, the roots effectively move to the left (the larger $\alpha$is, the further the non-dominant roots lie). Since we would like the contribution of the non-dominant roots to the overall response to be quickly fading and non-oscillatory, let $d_0 = \alpha^2\zeta^2{\omega_n}^2$so as to obtain two real roots. Substituting $d_1 = 2\alpha\zeta\omega_n$ and $d_0 = \alpha^2\zeta^2{\omega_n}^2$eq.(16),

$$(s^2 + 2\zeta\omega_n s + {\omega_n}^2)(s^2 + 2\alpha\zeta\omega_n s + \alpha^2\zeta^2{\omega_n}^2) = 0$$

$$s^4 + [2\zeta\omega_n(\alpha + 1)]s^3 + \{{\omega_n}^2[\alpha\zeta^2(\alpha + 4) + 1]\}s^2 + [2\alpha\zeta{\omega_n}^3(\alpha\zeta^2 + 1)]s + \alpha^2\zeta^2{\omega_n}^4 = 0 \quad (17)$$

Using second-order system approximation formulae we can obtain ζ, ω_n and other parameters like resonance frequencyω_r, peak magnitude$M_{p\omega}$and settling timeT_s.

The minimum damping ratio ζ for 15% overshoot can be obtained using

$$P.O. = 100e^{-\zeta\pi/\sqrt{1-\zeta^2}} \quad (18)$$

$$\zeta = 0.5169$$

Natural frequency,

$$\omega_n = \frac{\omega_B}{-1.1961\zeta + 1.8506}$$

$$\omega_n = 5.0960 \text{ rad/s} \quad (19)$$

(where bandwidth, $\omega_B$from our design specification $= 1\text{Hz} = 6.28 \text{ rad/s}$
Resonance frequency,

$$\omega_r = \omega_n\sqrt{1 - 2\zeta^2} \quad (20)$$

$$= 3.4774 \text{ rad/s}$$

Peak magnitude,

$$M_{p\omega} = \frac{1}{2\zeta\sqrt{1-\zeta^2}} \quad (21)$$

$$= 1.1300$$

Settling time (for 2% criterion),

$$T_s = 4\tau = \frac{4}{\zeta\omega_n}$$

$$= 1.52 \text{ sec} \quad (22)$$

Now substituting $\zeta = 0.5169$, $\omega_n = 5.0960$ rad/s and $\alpha = 100$, in eq. (17) and comparing with eq. (15), we have that:

From coefficients of s^3: $c = 481.5927$

s^2: $K_D = 8320.3452$

s: $a = 7.6749$

(constant terms) : $b = 37.6636$

The proportional and the integral gains are, of course:

$$K_P = K_D a = 63{,}857.8174$$

$$K_I = K_D b = 31{,}3374.1535$$

Now the controller, in the form$G_c(s) = \frac{K_D s^2 + K_P s + K_I}{s+c}$is

$$G_c(s) = \frac{8320.3452s^2 + 63857.8174s + 313374.1535}{s + 481.5927} \tag{23}$$

Now putting our controller parameters in eq.s (13) and (14),

$$L(s) = \frac{1913.6794s^2 + 14687.2980s + 72,076.0553}{0.04s^4 + 21.2837s^3 + 973.8173s^2 + 481.5927s} \tag{24}$$

$$T_1(s) = \frac{1913.6794s^2 + 14687.2980s + 72076.0553}{0.04s^4 + 21.2837s^3 + 2887.4967s^2 + 15168.8907s + 72076.0553} \tag{25}$$

and of course, the closed loop transfer function of the arm is

$$T_3(s) = \frac{5,741.0382s^2 + 44,061.894s + 216,228.1659}{0.04s^4 + 21.2837s^3 + 2887.4967s^2 + 15168.8907s + 72076.0553} \tag{26}$$

3.0 Results and Discussions

3.1 System Response and Stability

Using$T_1(s)$, we can plot the step response and magnitude plots.

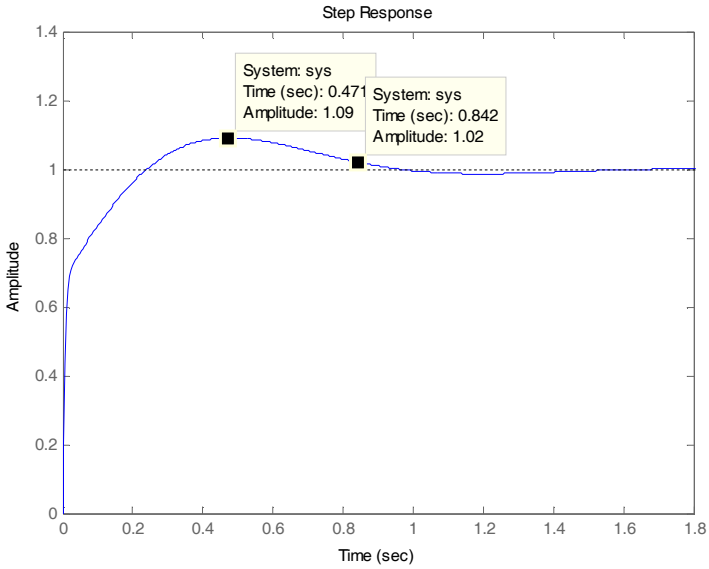

Fig. 3 Step Response of Each Joint

Rise Time: 0.1452 Overshoot: 9.1130
Settling Time: 0.8422 Undershoot: 0
Settling Min: 0.9021 Peak: 1.0911
Settling Max: 1.0911 Peak Time: 0.4747

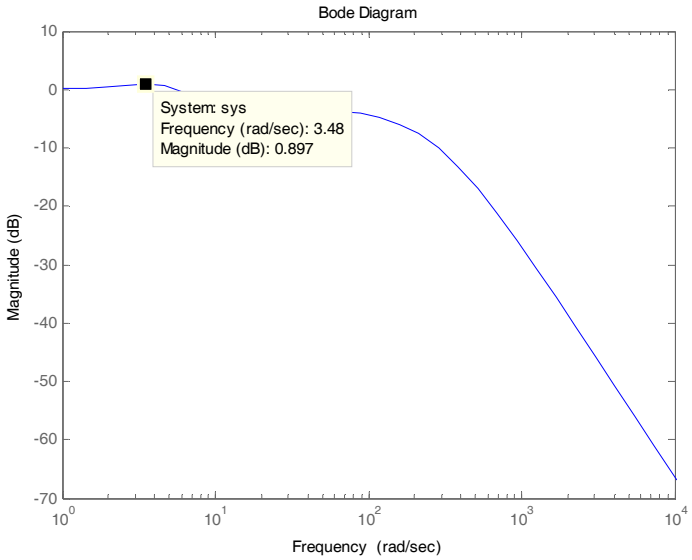

Fig. 4 Magnitude Plot of the Each Closed Loop System (Each Joint)

In the step response (fig. 3) we see that the system exhibits approximately 9.11% maximum overshoot which satisfies the design specification of below 15% as planned. In fig. 4, the peak magnitude is 0.90 (we were expecting 1.13).

3.2 Stability Test

No. of polesof $L(s)$ in the right hand$s$-plane see eq. (24):

$$s = 0$$
$$s = -0.5 - (2.8 \times 10^{-13})i$$
$$s = -50 + (2.3 \times 10^{-13})i$$
$$s = -481.6 - (2.8 \times 10^{-14})i$$

There are no poles to the right. Therefore, $P = 0$

No. of encirclements of the $-1 + j0$ point:

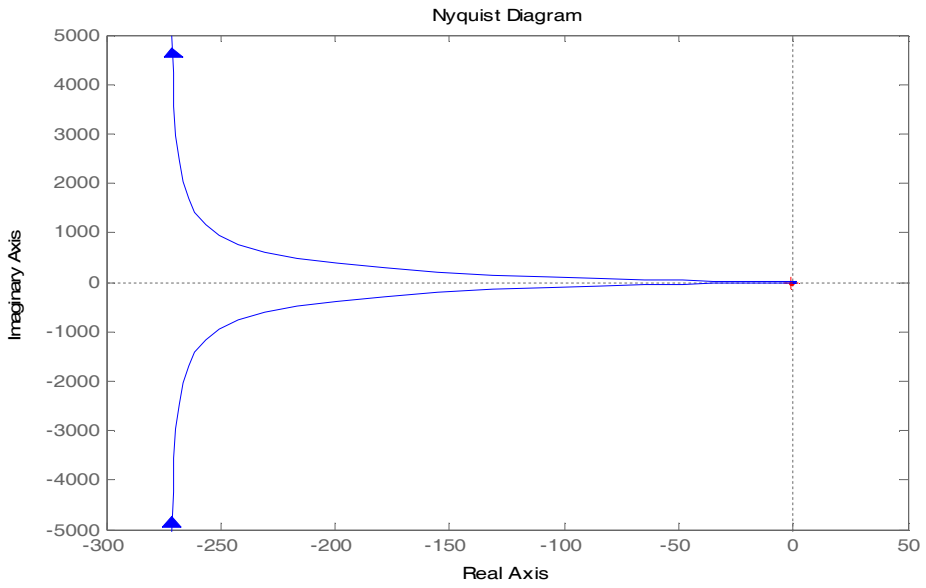

Fig. 5 Niquist Plot (Mapping for $L(s)$)

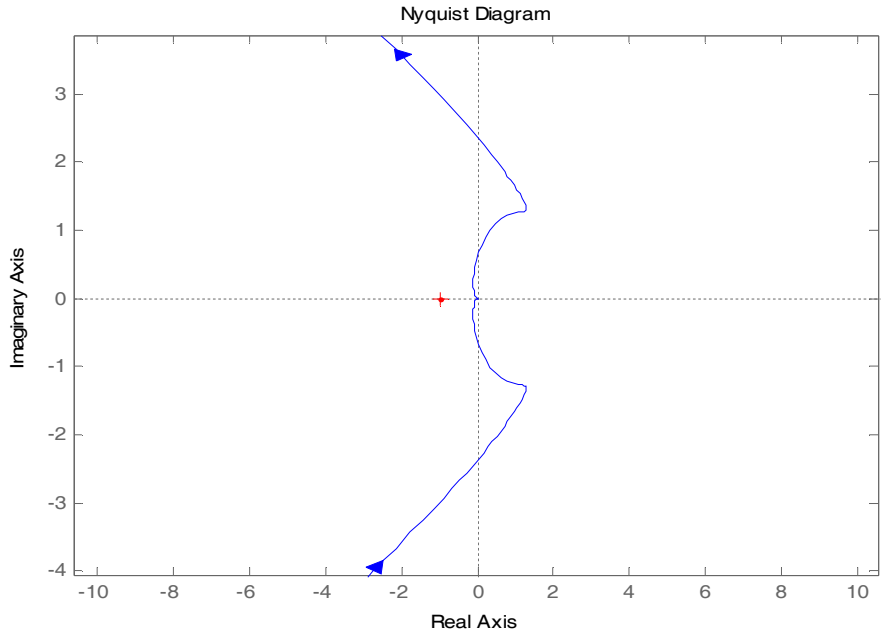

Fig. 6 Niquist Plot (Mapping for $L(s)$zoomed towards the origin)

In fig. 5 the branches go off towards infinity. However, because there is a pole at the origin (on the $j\omega$-axis) (see fig. 6), we can infer that the counterclockwise 180^{o} detour

around the origin in $s$yields a clockwise 180° detour in $L(s)$.The $-1+j0$ point is not encircled therefore $N=0$.

No. of unstable zeros of $F(s)$:

$$Z = N + P = 0 \qquad (27)$$

As a check, let us find the locations of the zeros by putting

$$F(s) = 1 + L(s) = 0 \qquad (28)$$

$$F(s) = \frac{0.04s^4 + 21.2837s^3 + 2{,}887.4967s^2 + 15{,}168.8907s + 72{,}076.0553}{0.04s^4 + 21.2837s^3 + 973.8173s^2 + 481.5927s} = 0 \qquad (29)$$

The zeros are$s = -2.63 \pm 4.36i$and$s = -263.41 \pm 0.26i$. (There are no zeros on the right).Therefore, the number of unstable zeros of $F(s)$, $Z = 0$

Inference: One of the conditions for stability according to Nyquist states that a feedback control system is stable if and only if the polar plot contour in the $L(s)$plane does not encircle the (-1,0) point $(N = 0)$when the number of poles of $L(s)$in the righthand$s$-plane is zero $(P = 0)$. Our feedback system is thus stable.

4.0. Conclusion

5.0 Recommendations

The following areas should be considered in future research

Nomenclature

RRR – three revolute joints

DOF – degree of freedom

$R(s)$, $E_a(s)$– the input voltage

$Y(s)$– output i.e. the desired position of the end-effecter's tip

$G(s)$–process transfer function of the actuator/link (field controlled DC servo)

$G_c(s)$–transfer function of the controller

$H(s)$– feedback transfer function

$L(s)$– loop gain

$T_L(s)$–loop transfer function

K_m – motor constant

b–equivalent coefficient of friction (of load and motor)

R_f– field winding resistance

τ_f–time constant for field circuit

τ_L –mechanical time constant

K – the gain $K = K_m/bR_f$

Z–no. of unstable zeros of $F(s) = 1 + L(s)$which are located on the right-hand *s*-plane

N–no. of encirclements of the $-1 + j0$ point

P–no. of poles of $L(s)$in the right hand*s*-plane

References

Farhan (2014)

Hossein and Hassan (2014) Katsuhiko Ogata: “Modern Control Engineering"Prentice-Hall.

Okubanjo A. A., Oyetola, O. K., Osifeko M. O., Olaluwoye O. O. and Alao, P. O., (2017): “Modeling of 2-DOF Robot Arm and Control”, FUTO Journal Series, 3(2), 80 – 92.

Richard C. Dorf and Robert H. Bishop: “Modern Control Systems", 9th Ed., Prentice-Hall, Inc. 2001)

Safdar, (2015). Takaya K: University of Saskatchewan, Electrical Engineering EE 480.3 Digital Control Review of AnalogController Design January, 2003